International Journal of Mechanical Engineering (IJME)
ISSN 2319-2240
Vol. 2, Issue 2, May 2013, 23-30

International Academy of Science, Engineering and Technology
Connecting Researchers; Nurturing Innovations

EFFECT OF SEMI-SOLID PROCESS ON MICROSTRUCTURE AND MECHANICAL PROPERTIES OF MEDIUM CARBON STEEL PRODUCED BY CONTINUOUS CASTING

NADER H. EL-BAGOURY[1,2], ADEL A. OMAR[3,4] & ALI A. EL-MASRY[3,5]

[1]Chemistry Department, Faculty of Science, TAIF University, El-Haweyah, El-Taif, Saudi Arabia

[2]Casting Technology Lab, Manufacturing Technology Department, CMRDI, Helwan, Cairo, Egypt

[3]Mechanical Engineering Department, Faculty of Engineering, TAIF University, El-Haweyah, El-Taif, Saudi Arabia

[4]Mechanical Engineering Department, Faculty of Engineering, Benha University, Benha , Egypt

[5]Production Engineering and Mechanical Design Engineering Department, Faculty of Engineering, Menofia University, Shebin El-Kom, Egypt

ABSTRACT

The effect of semi-solid process on the microstructure and mechanical properties of medium carbon steel (0.6% C) produced by continuous casting route was investigated. Both the microstructure and mechanical properties have been affected by semi solid process. The microstructure tends to consist mainly of martensite at the bottom of the casting. The volume fraction of martensite at the bottom of the semi solid casting is higher than that for the continuous casting. Carbides start to appear in the microstructure at the grain boundaries at higher levels of the vertical axis in both semi solid and continuous casting molds.

Hardness measurements for semi solid casting are higher than those for continuous casting especially at the bottom. Away from the bottom of two ingots, hardness gradually decreases to reach almost the same values at the top. Impact energy for semi solid casting is lower than that for the continuous casting.

KEYWORDS: Medium Carbon Steel, Semi-Solid, Continuous Casting, Microstructure, Mechanical Properties

INTRODUCTION

Due to its many economic advantages the continuous casting (CC) of steel has become more and more important during the last 40 years [1-5]. This process is mostly used for the production of a semi-fabricated strip, for cold rolling to foil-stock building sheet and can-stock. It is also used to cast endless wire bar stock. CC processes converts molten steel alloys directly into an endless coiled strip suitable for cold rolling or wire-bars for wire-drawing. It effectively eliminates the operations associated with traditional mould casting (discontinuous process) or D.C. casting (a semi-continuous process) and subsequent hot mill deformation [6-10].

Therefore the capital investment and operational costs are significantly lower than in a conventional production process. CC is the preferred casting method in many modern plants because it offers higher productivity. CC has been employed with increasing commercial success for steel as well as other metals [11-14].

Semi-solid metal (SSM) processing was invented more than 30 years ago at Massachusetts Institute of Technology [15]. It is a metal forming process that fills partially-solidified metal with globular structure in a mold, instead of casting with liquid metal. The characteristics of SSM are, for example, lower heat content than liquid metal, partially-solidified metal at the time of mold filling, higher viscosity than liquid metals, flow stress lower than for solid metals (de Figueredo, 2001) [16]. These characteristics offer several potential benefits for various applications.

SSM processing also allows thick and large components to be cast with die casting (de Figueredo, 2001) [16-19]. It is not practical to cast thick parts in conventional die casting, since so much heat needs to be extracted that the die life is significantly shortened and productivity is lower. SSM processing, thus, allows die casting to be used to produce a wider range of products [20-24].

In this investigation, two casting processes will be carried out to produce medium carbon steel ingots. The first ingot will be produced under conventional continuous casting process. The second will be produced using a complicated process; semi-solid processing will be used in addition to continuous casting process to produce the other ingot. The molten metal will be first poured into semi-solid plate, starting solidification process, and then poured into the continuous casting mould. However, in the first route of casting process, the molten medium carbon steel will be poured directly in the continuous casting mould.

The effect of casting route on microstructure and mechanical properties will be investigated. The influence of casting conditions on the grain size and the volume fraction of different phases in the microstructure will be studied. Moreover, the mechanical properties, such as hardness and impact strength, of the two ingots resulting from the two routes of casting will be compared.

EXPERIMENTAL WORK

The charge of medium carbon steel used in this investigation was heated in air atmosphere up to temperature of 1863 K, and then soaked for 10 min to allow the charge to attain the desired temperature. At 1840 K, the melted charge was removed from the furnace to the pouring system, which consisting of isolated box to regulate the melt temperature and speed-changeable motor to adjust the pouring rate.

At the desired temperature the melt charge is allowed to be poured over a cooling plate inclined at the known angle to the horizontal (10◦) with constant motor speed 600 rpm (constant pouring rate), and to flow into a continuous casting mold at the end of the cooling plate. Symbol (A) was given to the ingot produced by combine route through semi-solid and continuous casting, while symbol (b) was given to the other ingot produced through continuous casting technique only. The chemical composition of the both medium carbon steel alloys used in this work is shown in Table 1.

The dimensions of the ingots and the specimens' locations for both the microstructure and hardness investigations are shown in Figure 1.

The microstructure was examined by Meiji optical microscope fitted with a digital camera. The specimens for microstructure examination were prepared by standard metallographic procedures according to Standard ASTM E3-11 then etched in a solution of Nital (2% HNO_3).

Additionally, hardness measurements and impact toughness tests were carried out according to standard ASTM E348-11 using LECO Vickers Hardness Tester LV800AT and Computer Screen Display Impact Testing Machine, JBW 500, respectively.

Table 1: Chemical Composition of Medium Carbon Steel Alloys, Mass %

Symbol	Ingot	Elements									
		C	Si	Mn	P	S	Cr	Mo	Ni	Cu	Fe
A	SS + CC	0.59	0.51	0.87	0.04	0.02	0.07	0.01	0.02	0.14	Bal.
B	CC	0.64	0.43	0.65	0.06	0.03	0.20	0.03	0.05	0.20	Bal.

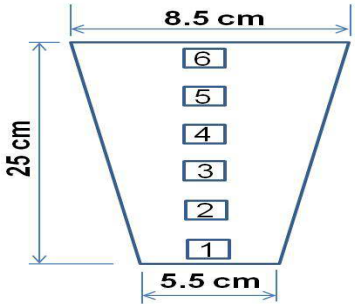

Figure 1: Schematic Illustration for the Ingot Dimensions and Specimens' Locations

RESULTS AND DISCUSSIONS

Microstructure

The microstructures for both A and B ingots at various levels along their vertical axes are shown in Figure 2.

At the bottom of the mold, the cooling rate is the highest because this region is in a contact with the copper chill, which is cooled by water. However, the region at the top of the mold has the lowest cooling rate as it is far from water cooling. For both A and B ingots, martensite is the predominant phase in microstructure at the bottom of the mold (highest cooling rate). The volume fraction of martensite phase is higher in A ingot than in B ingot. Martensite lath is clearer in A alloy than in B alloy as shown in Figure 2 (a) and (e). As the cooling rate decreases towards the top of the mold, the martensite phase starts to vanish from the microstructure. Bainite phase begins to appear in the microstructure in the medium levels of the mold at the expense of martensite in both ingots, Figure 2 (b) and (f). At the top of the mold (lowest cooling rate), pearlite and carbide phases are found in the microstructure, Figure 2 (c) and (d) in A ingot and (g) and (h) in B ingot.

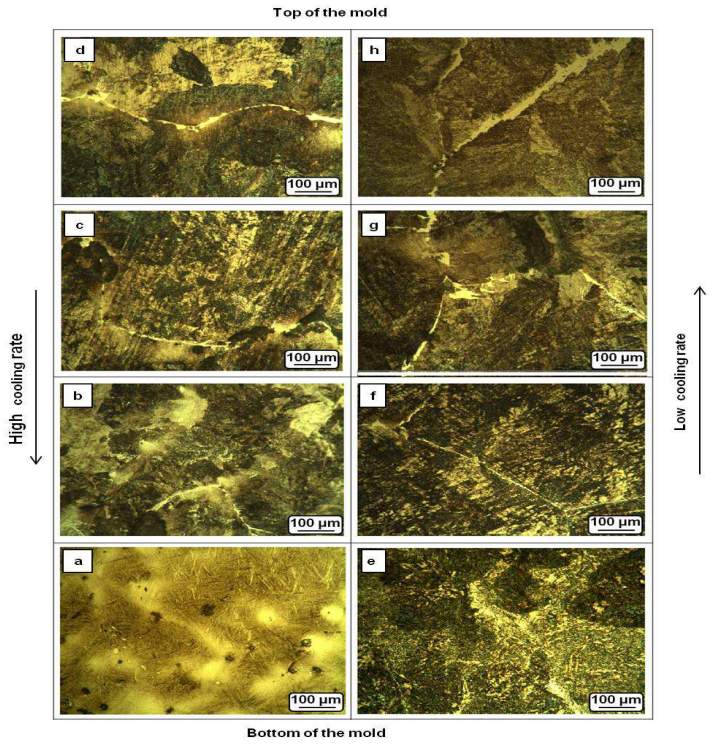

Figure 2: Microstructure of A and B Alloys along the Vertical Axis of the Mold. (a), (b), (c), (d) A Alloy and (e), (f), (g), (h) B Alloy

Because of the formation of carbides is a diffusion process, carbides found in the microstructures as the cooling rate decreases. At the highest cooing rate regions (bottom of the mold), carbides has not any chance to form and appear in microstructure, Figure 2 (a) and (e).

However, as the cooling rate decreases, carbides start to precipitate at the grain boundaries with thin thickness, Figure 2 (b) and (f). The thickness of carbides precipitate at the grain boundaries increases with more decrease in the cooling rate as shown in Figure 2 (c), (d), (g) and (h).

The grain size of A and B ingots was affected too by the cooling rate as shown in Figure 2. As the cooling rate decreases away from the mold bottom, the grain size decreases as well.

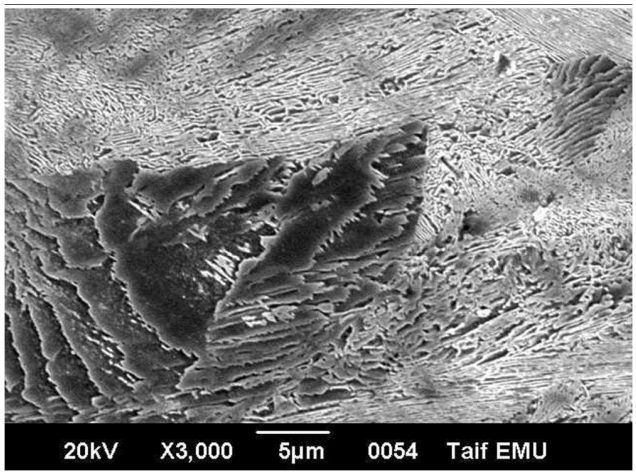

Figure 3: Pearlite Lamella in the Microstructure

Moreover, both bainite and pearlite were affected by the cooling rate at different levels along the vertical axis of the mold. As shown in Figure 3, pearlite lamella increases as the cooling rate decreases.

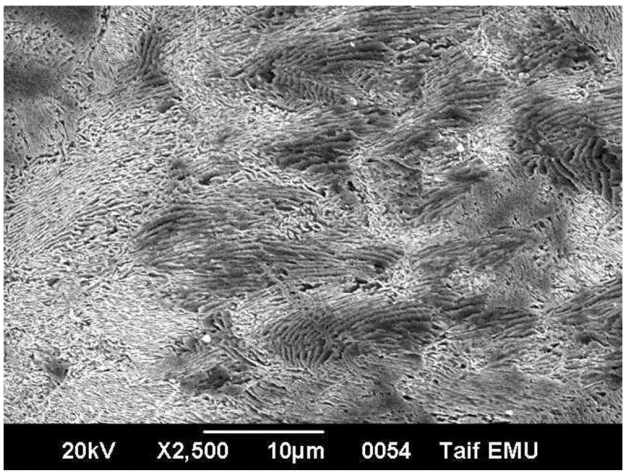

Figure 4: Pearlite Colonies in the Bainite Matrix

Figure 4 shows the existence of pearlite phase with different interior distance of lamella in a shape of colonies in the bainitic matrix.

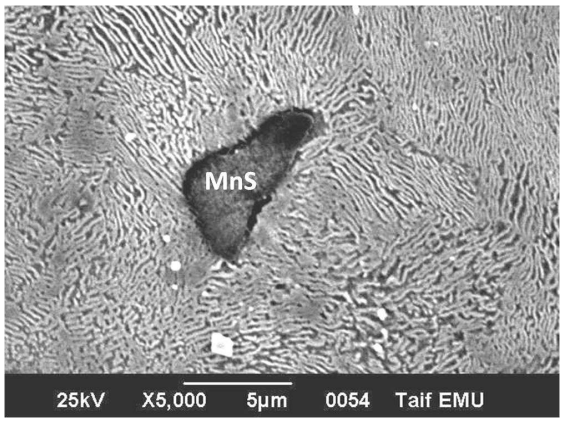

Figure 5: MnS Founded in the Microstructure of Specimen 6 in A Ingot

Figure 5 shows some non metallic inclusions of MnS type. This type of inclusions found embedded in the microstructure of A ingot at the slowest cooling rate specimen, which is specimen no. 6.

Mechanical Properties

Hardness Measurements

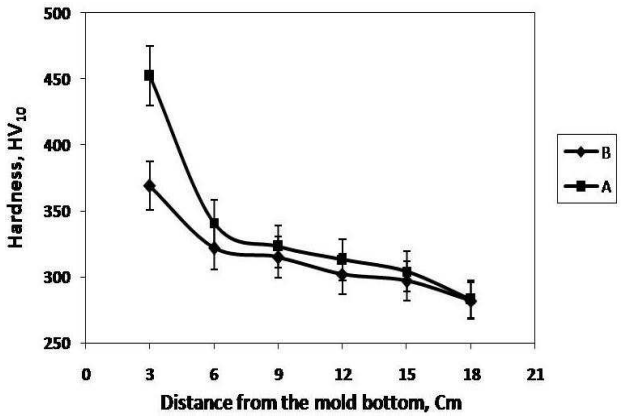

Figure 6: Hardness Measurements versus Distance from the Mold Bottom for Both Ingots

Hardness measurements for both A and B ingots along the vertical axis of the mold are shown in Figure 6. The hardness of A ingot is higher than that of B ingot at the same levels of the mold vertical axis. At the bottom of the mold, where cooling rate is higher, the difference in hardness between A and B ingots is high. This is probably due to the higher volume fraction of hard martensite in A ingot compared to that in B ingot as it can be seen from Figure 2. From the bottom of the mold towards to its top, the hardness values decrease gradually reaching to its lowest value at the top of the mold. This could be related to that the microstructure altered along the mold axis from martensite to bainite and pearlite.

Impact Strength

The impact properties of the investigated medium carbon steel ingots are shown in Table 2. The A ingot has impact strength lower than that for B ingot and consequently the toughness of B ingot is higher. These results could be related to two factors; first is the phases exist in the microstructure and second is the content of the gases and cavities included in different ingots that trapped and formed during solidification process.

From Figure 2, the amount of martensite phase in A alloy at the bottom of the mold is higher than that in B ingot. The martensite provides the strength whereas the ferrite provides toughness. Moreover, it seems that the content of gases

captured as well as the shrinkage cavities formed during the solidification process are higher in A ingot compared to ingot B. Both factors support the impact strength results shown in Table 2.

Table 2: Impact Properties of Medium Carbon Steel Ingots

Alloy	Impact Strength (Joules)
A	21
B	36

CONCLUSIONS

- Martensite volume fraction at the bottom of the mold in A ingot is higher than that in B ingot.
- Grain size is enlarged away from the mold bottom according to the cooling rate effects.
- Carbides appeared at the grain boundaries at higher levels of the mold axis and increased in thickness towards the top of the mold.
- Martensite found in the microstructure at the bottom of the mold transforms to bainite at medium levels of the mold axis then to pearlite at the top of the mold. Pearlite lamella increased away from the mold bottom as the cooling rate decreased.
- Generally hardness measurements of A ingot are higher than in B ingot and both gradually decreased towards the mold top. At the mold bottom the difference in hardness between A and B ingots is high and gradually decreased away from the mold bottom. Hardness for both A and B ingots reaches almost the same value at the top of the mold.
- Impact energy of A ingot is lower than that of B ingot. It could be due to the higher amount of gases entrapped and cavities in A ingot than in B ingot.

REFERENCES

1. Brimacombe J K 1993 Intelligent mould for continuous casting of billets. *Metall. Trans*. B24, pp. 917–928.
2. Darle T, Mouchette A, Nadif M, Roscini M, Salvadori D 1993 Hydraulic oscillation of the CC slab mould at Soleac Florange: First industrial results, future development. *Steelmaking Conference Proc*. (Warrendale, PA: Iron & Steel Soc.) vol. 76, pp. 209–218.
3. Harada S, Tanaka S, Misumi H 1990 A formation mechanism of transverse cracks on CC slab surface quality. South East Asian Iron & Steel Institute, pp. 26–32.
4. Hoedle H, Frauenhuber K, Moerwald K 1999 Advanced equipment for high performance casters. *Steelmaking Conference Proc*, vol. 82, pp. 141–151.
5. Kim K, Yeo T, Oh K B, Lee D N 1996 Effect of carbon & sulphur on longitudinal surface cracks. *Iron Steel Inst. Jpn. Int.* 36, pp. 284–292.
6. Ray S K, Mukhopadhyay B, Bhattacharyya S K 1996 Prediction of crack-sensitivity of concast slabs of AISI-430 stainless steel. *Iron Steel Inst. Jpn. Int.* 36, pp. 611–612.

7. Ray S K, Mukhopadhyay B, Das P C Nov. 1999 Effect of chemistry on solidification and quality of stainless steel. Presented at Annu. Tech. Mtg. of Indian Inst. Metals, Jamshedpur, pp. 14–17.

8. Saucedo I G 1991 Early solidification during continuous casting of steel. *Steelmaking Conference. Proc.* (Warrendale, PA: Iron & Steel Soc.) vol. 74, pp. 79–89.

9. Sen S, Mukhopadhyay B, Ray S K 1996 Continuous casting and hot rolling of AISI-310 stainless. *Steel India* 19, pp. 18–23.

10. Suzuki M, Mizukmi H, Kitagawa T, Kawakami K, Uchida S, Komatsu Y, 1991 Development of new mould oscillation mode for high-speed casting. *Iron Steel Inst. Jpn. Int.* 31, pp. 254–261.

11. Szekeres E S 1996 Overview of mould oscillation in continuous casting. *Iron Steel Eng.* July, pp. 29–37.

12. Tada K, Birat J P, Riboud P, Larrecq M, Hackel H 1984 Modelling of slag rim formation and pressure in molten flux near the meniscus. *Trans Iron Steel Inst. Jpn.* B24, pp.382–387.

13. Takeuchi E, Brimacombe J K 1984, The formation of oscillation marks in the continuous casting of steel slabs. *Metall. Trans.* B15, pp. 493–509.

14. Takeuchi S, Miki Y, Itoyama S, Kobayishi K, Sorimachi K, Sakuraya T 1991 Control of oscillation mark formation during continuous casting. *Steelmaking Conference Proc*. (Warrendale, PA: Iron & Steel Soc.) vol. 74, p. 303.

15. Wolf M M 1986 Strand surface quality of stainless steel. *Ironmaking Steelmaking* 13, pp. 248– 259.

16. de Figueredo A, Ed. 2001. Science and Technology of Semi- Solid Metal Processing. The North American Die Casting Association, U.S.A.

17. Flemings, M.C. 1971, Solidification Processing, McGraw- Hill, Inc., New York, U.S.A., pp. 146-154.

18. Flemings MC, Yurko JA, Martinez RA. Semi-solid forming: our understanding today and its implications for improved processes. Solidification Processes and Microstructures: A Symposium in Honor of Wilfried Kurz as held at the Minerals, Metals, and Materials Society Annual Meeting, Charlotte, NC, U.S.A., March 14-18, 2004, pp. 3-14.

19. http://www.ubemachinery.com/diecasting.html. [March 2, 2006].

20. Jorstad J.L. SSM Processes – An Overview. Proceedings of the 8th International Conference on Semi-Solid Processing of Alloys and Composites, Limassol, Cyprus, September, 2004, pp.21–23.

21. Ph.D. Thesis, Massachusetts Institute of Technology, Cambridge, MA, U.S.A.

22. Spencer, D.B. 1971. Rheology of liquid-solid mixtures of lead-tin. Ph.D. Thesis, Massachusetts Institute of Technology, Cambridge, MA, U.S.A.

23. Wannasin J., Martinez R.A., Flemings M.C. 2006. Grain refinement of an aluminum alloy by introducing gas bubbles during solidification. Scripta Materialia. 55, pp. 115-118.

24. Yurko J., Martinez A., Flemings M. SSRTM: The Spheroidal Growth Route to Semi-Solid Forming. Proceedings of the 8th International Conference on Semi-Solid Processing of Alloys and Composites, Limassol, Cyprus, September, 2004,pp. 21-23.